Available online at www.sciencedirect.com
ScienceDirect
Optics Communications xxx (2007) xxx–xxx
OPTICS COMMUNICATIONS
www.elsevier.com/locate/optcom

Lateral resolution improvement in two-photon excitation microscopy by aperture engineering

Partha Pratim Mondal [a,*], Alberto Diaspro [b,c,d]

[a] International Center for Theoretical Physics, Trieste, Italy
[b] IFOM-LAMBS-MicroScoBiO, University of Genova, Italy
[c] Department of Physics, University of Genova, Italy
Q3 [d] Institute of Biophysics, CNR, Italy

Received 16 June 2007; received in revised form 12 August 2007; accepted 13 September 2007

Abstract

A technique for resolution improvement in two-photon excitation (2PE) fluorescence microscopy based on radially-symmetric annular binary filter (consist of central circular aperture and a concentric peripheral annulus) is proposed. Resolution improvement is achieved by engineering the aperture of the objective lens in a way so as to enhance high spatial frequencies. The structure of the electromagnetic field in the regions of focus and nearby regions are determined. The central lobe of the time-averaged electric energy density is considerably reduced for both linearly- and circularly-polarized illuminated light. An impressive combined comparative percentage improvement of 40% and 53.71% both at low ($\alpha = 30$) and high ($\alpha = 60$) aperture angle is obtained for linearly-polarized light. Proposed aperture engineering technique complements conventional, confocal, two-photon fluorescence microscopy, and may facilitate working at low-to-medium magnifications and large free-working distances.

The resolution of an optical microscope is ultimately limited by Abbe's diffraction criterion [1]. The objective lens generates a point-spread-function (PSF) that produces airy-disk intensity pattern (concentric rings of successively decreasing maximum and minimum intensity) which is due to the interference between the diffracted wavefronts [2]. The half of the diameter of the first dark ring (d_{dark}) of the airy-disk sets the limit for smallest resolvable distance (r) in the lateral plane, i.e., $r = \frac{1}{2} d_{\mathrm{dark}} \approx \frac{\lambda}{2n\sin\alpha}$ where, $NA = n\sin\alpha$ is the numerical aperture of the objective lens and λ is the wavelength of illuminated light.

Currently few methods exists for resolution improvement in single- and two-photon excitation microscopy. Resolution improvement techniques such as 4PI and stimulated emission depletion (STED) can resolve objects beyond diffraction limit but require complex optical configuration and instrumentation [3]. In far-field domain, photoactivated localization microscopy has shown promising resolution improvement [4]. Gustafsson has demonstrated a simple lateral resolution improvement by using spatially structured illumination in a wide-field fluorescence microscope [5]. Heintzmann et al. have developed nonlinear patterned excitation microscopy for achieving a substantial improvement in resolution by deliberate saturation of the fluorophore excited state [6]. Several deconvolution methods have shown impressive improvement in signal-to-noise (SNR) ratio and resolution [7–11]. Most of these advanced techniques require complex experimental setup and imposes several limitations on in-depth imaging and saturation due to fluorescence from off-focus planes. Other approach shrinks the PSF by a phase pattern in the entrance pupil of the lens but the side lobes makes it impractical [12]. Resolution improvement in confocal 2PE microscopy is very much in demand because of the penetration depth it provides and minimal photon-fluorophore interaction from off-focus planes. However, the lateral and axial resolution severely suffers because of the

* Corresponding author.
E-mail address: partha@fisica.unige.it (P.P. Mondal).

0030-4018/$ - see front matter © 2007 Elsevier B.V. All rights reserved.
doi:10.1016/j.optcom.2007.09.067

requirement of double wavelength for 2PE microscopy. This is directly evident from Abbe's diffraction criterion as well [1].

In this letter, we propose a simple microscopy technique for lateral resolution improvement in confocal 2PE fluorescence microscopy. This is achieved by allowing light from the central and peripheral annulus of the objective lens. As a result, a compact central lobe along with very weak airy disks is formed at the objective focus. Simulated results show impressive improvement in the lateral resolution. It should however be noted that similar studies mainly focussed on PSF engineering in single-photon excitation microscopy have been reported by Neil et al. [13], Hell [14], Botcherby et al. [15] and Wilson and Sheppard [16]. Hell et al. [17] has also carried out similar study in two-photon excitation microscopy. Additionally, Martynez-Corral et al. have demonstrated the use of annular binary filters for increasing the 3D resolution capacity of confocal scanning microscopy in bright field mode [18].

In a confocal 2PE fluorescence microscope, the normalized excitation PSF for linearly-polarized light in the focal region is given by

$$h_{\mathrm{exc},\Delta\alpha} = |\overline{E}_{\mathrm{exc},\Delta\alpha}|^4 = [|I_0|^2 + 4|I_1|^2\cos^2(\phi) + |I_2|^2 + 2\cos(2\phi)\mathrm{real}(I_0 I_2^*)]^2, \quad (1)$$

and for randomly or circularly-polarized light, the normalized PSF reduces to

$$h_{\mathrm{exc},\Delta\alpha} = [|I_0|^2 + 2|I_1|^2 + |I_2|^2]^2, \quad (2)$$

where, I_0, I_1 and I_2 are integrals over the objective lens aperture as defined in Ref. [19]. The parameter ϕ is the angle between the incident electric field and direction of observation; $\Delta\alpha$ is the total illumination aperture angle.

The detection of fluorescent light is assumed to be randomly polarized. Hence the detection PSF is given by

$$h_{\mathrm{det}} = |\overline{E}_{\mathrm{det}}|^2 = |I_0|^2 + 2|I_1|^2 + |I_2|^2. \quad (3)$$

So, the confocal 2PE PSF (h_{TPE}) is the product of the excitation PSF ($h_{\mathrm{exc},\Delta\alpha}$) and detection PSF ($h_{\mathrm{det}}$), i.e.,

$$h_{\mathrm{TPE}} = |\overline{E}_{\mathrm{exc},\Delta\alpha}|^4 \times |\overline{E}_{\mathrm{det}}|^2 = \begin{cases} [|I_0|^2 + 4|I_1|^2\cos^2(\phi) + |I_2|^2 + 2\cos(2\phi)\mathrm{real}(I_0 I_2^*)]^2 \times [|I_0|^2 + 2|I_1|^2 + |I_2|^2], & \text{for linear polarized light,} \\ [|I_0|^2 + 2|I_1|^2 + |I_2|^2]^3, & \text{for circular polarized light.} \end{cases} \quad (4)$$

In the proposed aperture engineering (AE) approach the excitation wavefronts emerging from both the slits, i.e., central circular slit of angle $\Delta\alpha_1$ and annular slit of angle $\Delta\alpha_2$ gives the effective PSF of the proposed technique at the focal plane (see Fig. 1). The PSF for the proposed 2PE excitation scheme is

$$h_{\mathrm{AE}} = (|\overline{E}_{\mathrm{exc},\Delta\alpha_1} + \overline{E}_{\mathrm{exc},\Delta\alpha_2}|^2)^2 \times |\overline{E}_{\mathrm{det}}|^2, \quad (5)$$

where, $|\overline{E}_{\mathrm{exc},\Delta\alpha_i}|, i = 1, 2$ are given by Eq. (1) for linearly- and Eq. (2) for circularly-polarized light; $|\overline{E}_{\mathrm{det}}|$ is given by (3). As a consequence of the superposition of fields emerging from the annular and central circular slit, the resulting PSF is a compact central bright spot accompanied by fading circular rings. This is because the proposed radially-symmetric annular binary filter attenuates the intermediate frequencies, whereas alleviates high frequencies at the expense of diminution of low frequencies [18,20]. Nevertheless, the general characteristic of annular filters for improving the lateral resolution at the expense of axial resolution is well-known in confocal microscopy [15,16,18]. It should however be noted that, the accompanying side lobes are substantially reduced due to the quadratic dependence of intensity along the optical axis in TPE microscopy. Further reduction in side lobes can be achieved by deconvolution [7,8] and Bayesian reconstruction techniques [9,11].

The simulated experimental setup is schematically shown in Fig. 1. The 3D PSF is decomposed into $128 \times 128 \times 128$ pixels. The lateral sampling is 30 nm and the axial sampling is 90 nm. A light of wavelength 976 nm is used for two-photon excitation scheme. In the present setup, we propose to work with both linearly- and circularly-polarized light for excitation. Hence, the Boivin–Wolf PSF (BW-PSF) [19] for linearly-polarized light is given by (4) with $h_{\mathrm{exc},\Delta\alpha}$ and h_{det} given by (1) and (3), respectively. The BW-PSF for circularly-polarized light is given by (4) with $h_{\mathrm{exc},\Delta\alpha}$ and h_{det} given by (2) and (3), respectively. The proposed aperture engineering based PSF (AE-PSF) is given by (5), with excitation PSF given by (1) for linearly-polarized light and (2) for circularly-polarized light whereas the detection PSF is given by (3). We have chosen to work with a slit illumination angle of $\Delta\alpha_1 = \Delta\alpha_2 = 5°$ (see Fig. 1). In our simulation studies, light is allowed to pass through slit angles $\Delta\alpha_1$ and $\Delta\alpha_2$. Computationally, the integration on the integrals I_0, I_1 and I_2 are carried over the objective lens aperture angles $\Delta\alpha_1$ and $\Delta\alpha_2$, i.e., $[\int_{\Delta\alpha_1} I_{(0,1,2)} + \int_{\Delta\alpha_2} I_{(0,1,2)}]$ for the $I_{(0,1,2)}$ integrals [19].

The 2PE PSF for both BW and AE approach are shown in Fig. 2. BW- and AE-PSF for linearly-polarized light at different aperture angle (30, 45, 60) are shown in Fig. 2a–c and d–f, respectively. The corresponding BW- and AE-PSF for circularly-polarized light are shown in Fig. 2g–i and j–l, respectively. AE-PSF is compact as compared to BW-PSF with negligibly small airy disks as evident from Fig. 2. Comparison of linearly- and circularly-polarized light shows ϕ-dependence in the PSF (see Fig. 2). The corresponding contour plots of the intensity (time-averaged electric energy density) along the lateral focal plane are also

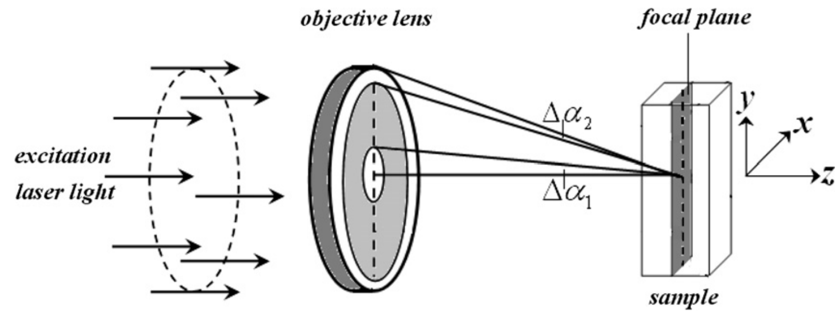

Fig. 1. A simplified schematic diagram of the proposed AE system.

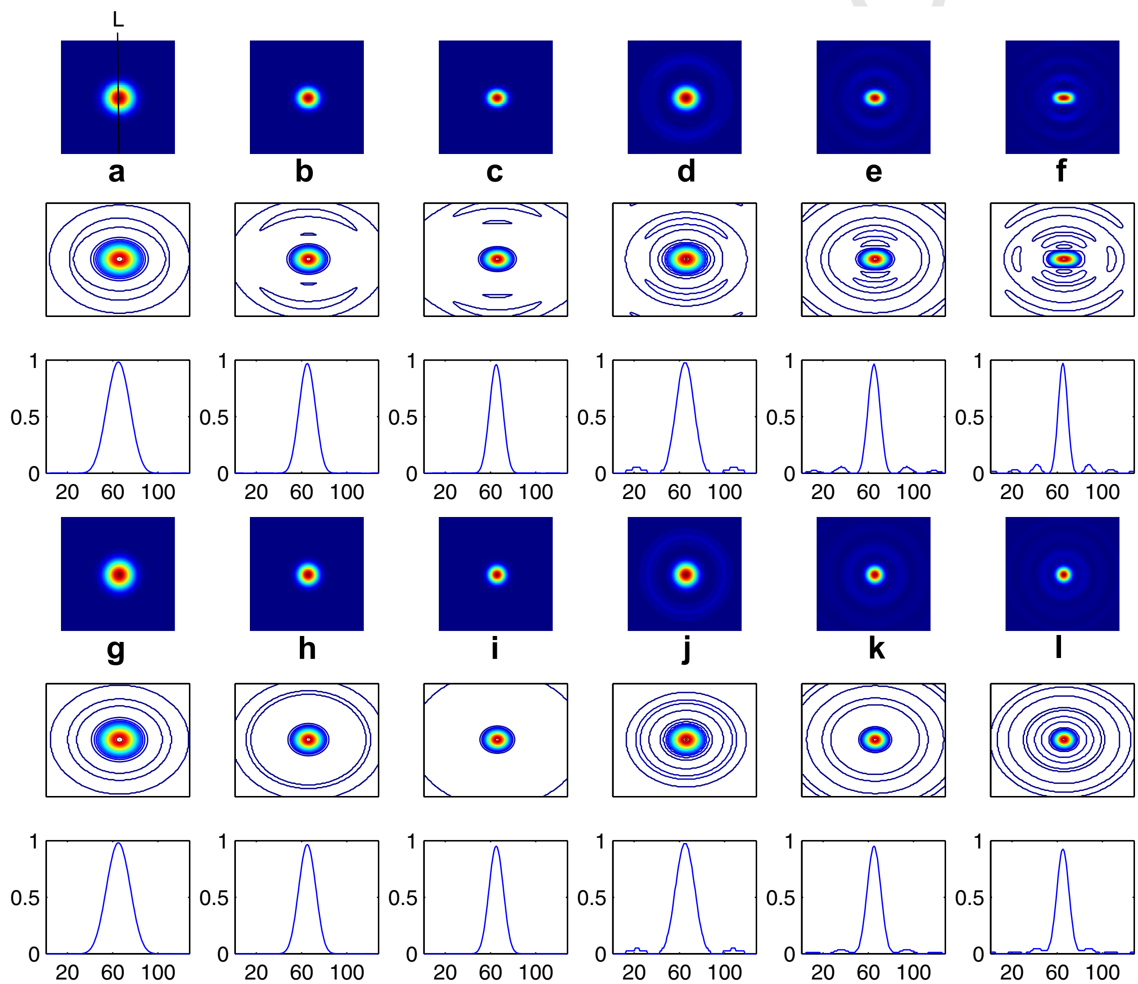

Fig. 2. BW-PSF and AE-PSF for linearly-polarized light at aperture angles (30, 45, 60) is shown in (a–c) and (d–f), respectively. BW-PSF and AE-PSF for the case of circularly-polarized light is shown in (g–i) and (j–l), respectively. Below each figure are shown time-averaged electric energy density map and the intensity distribution along vertical central line L.

shown below each PSF. AE approach deforms the structure of electric energy density near the center of PSF at the expense of compact central lobe. For better understanding the behavior of accompanying side lobes, we have shown intensity plots along the central vertical line L through each PSF in Fig. 2. The line plots show that the side-lobe intensity is less than 5% and hence can be neglected compared to the central lobe. The side lobes generated by the proposed technique are substantially small when compared to confocal microscopy. Using a similar filter, a transverse side-lobe of about 11% is reported in Ref. [18]. For the characterization of central lobe, normalized intensity plots along the lateral (x- and y-) direction for aperture angle 45° is shown in Fig. 3. Although in each case we have normalized the intensity at the focal point to be unity for ease of comparison, it is important to realize that this value depends on the filter used. BW-PSF(L) and BW-PSF(C) represent BW-PSF for linear and circular polarized

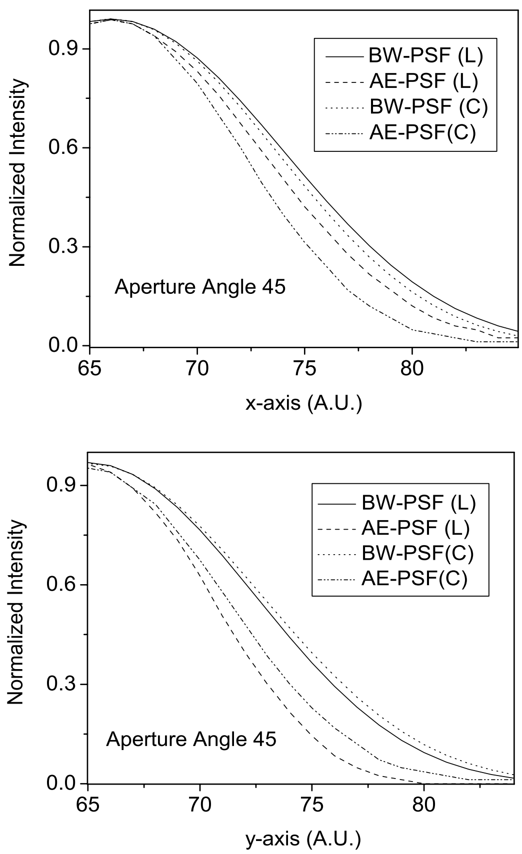

Fig. 3. Lateral sections (x- and y-axis) through the experimental point-spread functions of Fig. 2 for $\alpha = 45$.

light. Similar notation for AE-PSF is used. Another important parameter is the optical transfer function (OTF) which gives the spatial frequency content. Careful inspection of OTF in Fig. 4 shows a dramatic change in the lateral bandwidth of spatial frequency content of AE-PSF as compared to BW-PSF. This mimics the possibility of tailoring desired OTF by suitably engineering the aperture of the lens.

Table 1 shows the comparative full-width-half-maximum values of BW- and AE-PSF along the lateral axes (x- and y-axis) in terms of percentage improvement. Percentage improvement is defined as

$$PI_{\mathrm{FWHM}} = \frac{d_{\mathrm{BW}} - d_{\mathrm{AE}}}{d_{\mathrm{BW}}} \times 100\%, \tag{6}$$

where, d_{BW} and d_{AE} are the FWHM for BW- and AE-PSF in the focal plane. We have compared FWHM along both the lateral axis (x-axis, $PI^{(x)}_{\mathrm{FWHM}}$ and y-axis, $PI^{(y)}_{\mathrm{FWHM}}$) for linear and circular polarized light. A substantial reduction of the central lobe of AE-PSF as compared to BW-PSF is pre-

Table 1
Description of $PI_{\mathrm{FWHM}}(\%)$

Polarization	Lateral axis	Aperture angle		
		$\alpha = 30$	$\alpha = 45$	$\alpha = 60$
Linear	(x)	24	23.52	6.66
Linear	(y)	16	10.52	47.05
Circular	(x)	24	11.76	13.33
Circular	(y)	24	11.76	13.33

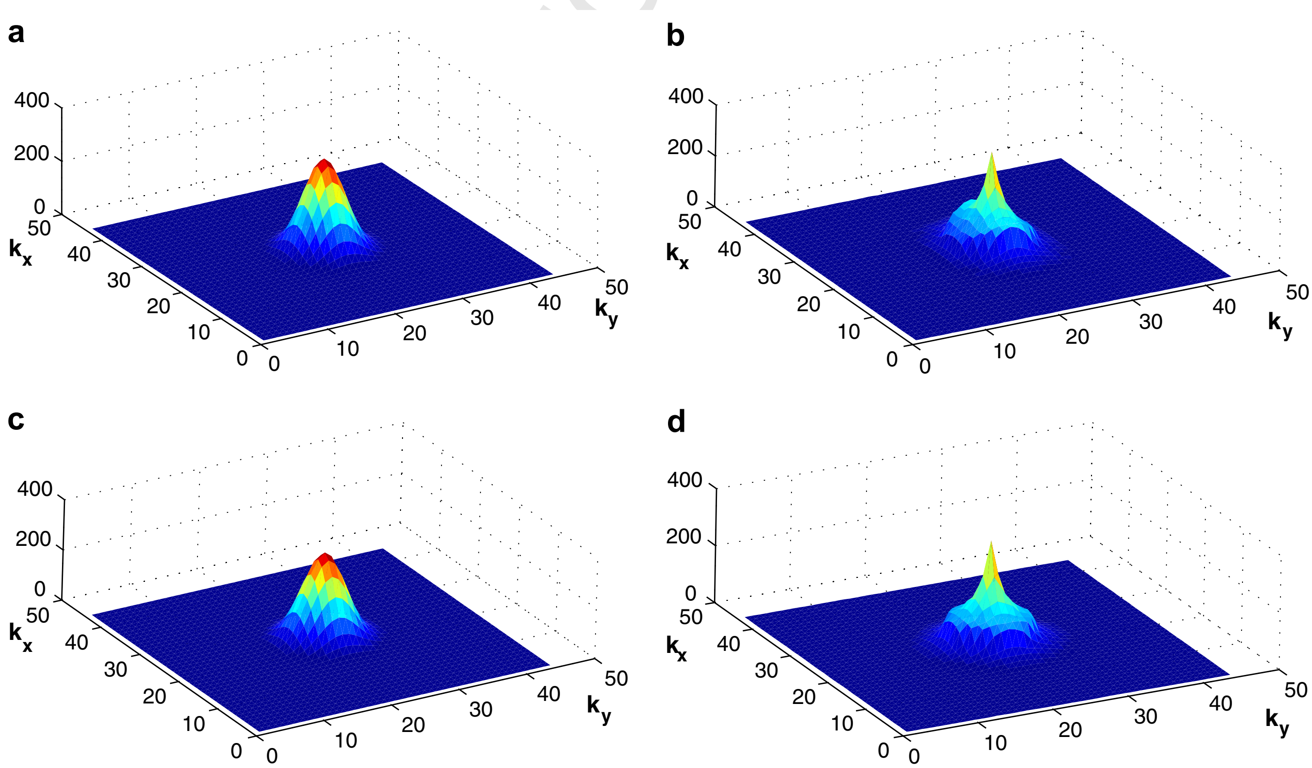

Fig. 4. Optical transfer function at $\alpha = 45$ of (a) BW-PSF, (b) AE-PSF for linearly-polarized light; and (c) BW-PSF, (d) AE-PSF for circularly-polarized light.

Please cite this article in press as: P.P. Mondal, A. Diaspro, Opt. Commun. (2007), doi:10.1016/j.optcom.2007.09.067

dicted by the FWHM values. Overall a combined FWHM ($PI^{(x)}_{\mathrm{FWHM}} + PI^{(y)}_{\mathrm{FWHM}}$) of 40%, 34.04% and 53.71% for aperture angle 30, 45 and 60 degree are, respectively obtained along the lateral plane using linearly-polarized light. Similarly for circularly-polarized light, a combined FWHM of 48%, 23.52% and 26.66% are obtained for aperture angle 30, 45 and 60 degree. Absence of any negative PI_{FWHM} shows an overall improvement in lateral resolution.

In this letter, we propose resolution improvement in 2PE fluorescence microscopy by aperture engineering technique. This is achieved by engineering the aperture so that the wavefronts emerging from the central circular aperture and concentric annulus of the objective interferes. Such a symmetric binary filter results in a compact PSF at the focus of the objective lens. The proposed filter improves resolution by alleviating high frequencies. It should be noted that the central lobe of proposed AE-PSF is accompanied by weak side lobes. However, the reduction in side lobes intensity is impressive using the proposed technique. Overall an improvement in FWHM of along the lateral axes is predicted by the simulation studies. Proposed technique could be useful for analyzing thin biological samples at large free-working distances. This technique may find applications in wide-field and two-photon excitation microscopy.

Acknowledgements

Partha Pratim Mondal thanks International Center for Theoretical Physics, Trieste, Italy for ICTP Fellowship. Alberto Diaspro acknowledge grants from IFOM, Milan, Italy.

References

[1] E. Abbe, Abhandlungen über die theorie des mikroskops, Gesammelte Abhandlungen, Fischer, Jena, 1904.
[2] H.E. Keller, in: J.B. Pawley (Ed.), Handbook of Biological Confocal Microscopy, third ed., 2006, p. 145 (Chapter 7).
[3] S.W. Hell, Science 316 (2007) 1153.
[4] E. Betzig, G.H. Patterson, R. Sougrat, O.W. Lindwasser, S. Olenych, J.S. Bonifacino, M.W. Davidson, J. Lippincott-Schwartz, H.F. Hess, Science 313 (2006) 1642.
[5] M.G.L. Gustafsson, J. Microsc. 198 (2000) 82.
[6] R. Heintzmann, T. Jovin, C. Cremer, J. Opt. Soc. Am. A 19 (2002) 1599.
[7] M. Schrader, S.W. Hell, H.T.M. van der Voort, J. Appl. Phys. 84 (1998) 4033.
[8] P.E. Hanninen, S.W. Hell, J. Salo, E. Soini, C. Cremer, Appl. Phys. Lett. 66 (1995) 1698.
[9] G. Vicidomini, P.P. Mondal, A. Diaspro, Opt. Lett. 31 (2006) 3582.
[10] A. Diaspro, S. Annunziata, M. Robello, Microsc. Res. Tech. 51 (2000) 464.
[11] P.P. Mondal, G. Vicidomini, A. Diaspro, J. Appl. Phys. 102, in press.
[12] G. Toraldo di Francia, Nuovo Cimento 9 (Suppl. 9) (1952) 426.
[13] M.A.A. Neil, R. Juskaitis, T. Wilson, Z.J. Laczik, V. Sarafis, Opt. Lett. 25 (2000) 245.
[14] S.W. Hell, Opt. Commun. 106 (1994) 19.
[15] E.J. Botcherby, R. Juskaitis, T. Wilson, Opt. Commun. 268 (2006) 253.
[16] T. Wilson, C. Sheppard, Theory and Practice of Scanning Optical Microscopy, Academic Press Inc., London and NY, 1984.
[17] S.W. Hell, P.E. Hanninen, A. Kuusisto, M. Schrader, E. Soini, Opt. Commun. 117 (1995) 20.
[18] M. Martynez-Corral, P. Andres, C.J. Zapata-Rodryguez, M. Kowalczyk, Opt. Commun. 165 (1999) 267.
[19] A. Boivin, E. Wolf, Phys. Rev. 138 (1965) B1561.
[20] G.R. Boyer, Opt. Acta 30 (1983) 807.

Please cite this article in press as: P.P. Mondal, A. Diaspro, Opt. Commun. (2007), doi:10.1016/j.optcom.2007.09.067